crystals

MDPI

Article

Coordination Ability of 10-EtC(NHPr)=HN-7,8-$C_2B_9H_{11}$ in the Reactions with Nickel(II) Phosphine Complexes

Marina Yu. Stogniy [1,*], Svetlana A. Erokhina [1], Kyrill Yu. Suponitsky [1,2], Igor B. Sivaev [1] and Vladimir I. Bregadze [1]

[1] A.N. Nesmeyanov Institute of Organoelement Compounds, Russian Academy of Science, 28 Vavilov Street, 119991 Moscow, Russia; hoborova.svetlana@yandex.ru (S.A.E.); kirshik@yahoo.com (K.Y.S.); sivaev@ineos.ac.ru (I.B.S.); bre@ineos.ac.ru (V.I.B.)

[2] Basic Department of Chemistry of Innovative Materials and Technologies, G.V. Plekhanov Russian University of Economics, 36 Stremyannyi Line, 117997 Moscow, Russia

* Correspondence: stogniymarina@rambler.ru or stogniy@ineos.ac.ru

Abstract: The complexation reactions of *nido*-carboranyl amidine 10-PrNHC(Et)=HN-7,8-$C_2B_9H_{11}$ with different nickel(II) phosphine complexes such as [$(PR_2R')_2NiCl_2$] (R = R′ = Ph, Bu; R = Me, R′ = Ph) were investigated. As a result, a series of novel half-sandwich nickel(II) π,σ-complexes [3-R′R_2P-3-(8-Pr*N*=C(Et)NH)-*closo*-3,1,2-$NiC_2B_9H_{10}$] with the coordination of the carborane and amidine components was prepared. The acidification of obtained complexes with HCl led to the breaking of the Ni-N bond with formation of nickel(II) π-complexes [3-Cl-3-R′R_2P-8-PrNH=C(Et)NH-*closo*-3,1,2-$NiC_2B_9H_{10}$]. The crystal molecular structure of [3-Ph_3P-3-(8-Pr*N*=C(Et)NH)-*closo*-3,1,2-$NiC_2B_9H_{10}$] was determined by single crystal X-ray diffraction.

Keywords: boron chemistry; *nido*-carborane; nitrilium derivatives; nickel(II) half-sandwich complexes; synthesis; structure

Citation: Stogniy, M.Y..; Erokhina, S.A.; Suponitsky, K.Y..; Sivaev, I.B.; Bregadze, V.I. Coordination Ability of 10-EtC(NHPr)=HN-7,8-$C_2B_9H_{11}$ in the Reactions with Nickel(II) Phosphine Complexes. *Crystals* **2021**, *11*, 306. https://doi.org/10.3390/cryst11030306

Academic Editor: Alexander Kirillov

Received: 28 February 2021
Accepted: 16 March 2021
Published: 19 March 2021

1. Introduction

The dicarbollide dianion [7,8-$C_2B_9H_{11}$]$^{2-}$, which is the deprotonated form of 7,8-dicarba-*nido*-undecaborate anion [7,8-$C_2B_9H_{12}$]$^-$ (*nido*-carborane), is known as the inorganic isolobal analogue of the cyclopentadienyl ligand. This makes it the perfect building block in complexation reactions with a wide range of transition metals [1–3]. The possibility to substitute hydrogen atoms at the carbon and boron vertices of the carborane cage with various functional groups [4] makes it possible to vary the properties of ligands based on *nido*-carborane by combining the properties of the *nido*-carborane nest with the properties of an exo-polyhedral substituent. One of the most interesting and promising tasks in this area is the synthesis of heterobifunctional *nido*-carborane-based ligands, that can give a firm bound to capture the metal center along with a weak bond, temporarily protecting a metal coordination site. This allows users to obtain labile complexes of transitional metal representing a promising new type of catalysts [5–10] and molecular switches [11,12]. There are several examples of such stable metal complexes based on *nido*-carborane with a side substituent coordinated through oxygen or nitrogen [5–8,13–15]. The utility of such bifunctional ligand systems with the nitrogen donor atom in the side chain has been demonstrated by the complexation of [7-Me_2NCH_2-7,8-$C_2B_9H_{11}$]$^-$ with metals such as nickel [16], iron [17], rhuthenium [17], titanium, zirconium, and hafnium [18,19]. In all cases, the intramolecular coordination of the dimethylamino group of the side substituent with the complexing metal was observed. The possibility of disrupting this coordination in the nickel(II) complexes by displacing the amino group with other soft ligands, such as triethylphosphine or *tert*-butylisocyanide, has been shown [16].

Earlier, we prepared a series of *nido*-carborane-based amidines 10-R$(CH_2)_n$NHC(Et)=HN-7,8-$C_2B_9H_{11}$ using the reaction of nucleophilic addition of amines to the 10-propionitrilium

derivative of *nido*-carborane [20]. Therefore, it was of interest to study the possibility of using obtained amidines in the complexation reactions, where *nido*-carborane itself represents a firm π-acceptor and amidine nitrogen can act as an intramolecular protecting group. In this contribution we report synthesis of a series of new metallacarboranes by the reactions of *nido*-carborane-based amidine 10-PrNHC(Et)=HN-7,8-$C_2B_9H_{11}$ with nickel(II) phosphine complexes [$(R_2R'P)_2NiCl_2$].

2. Results and Discussion

Recently, we have shown the ease and simplicity of the modification of the *nido*-carborane moiety via nucleophilic addition reactions of various nucleophiles to the highly activated nitrilium group -N^+≡C-R attached to the cluster [20–22]. The nucleophilic addition of aliphatic and aromatic amines to the 10-propionitrilium derivative of *nido*-carborane (10-EtC≡N-7,8-$C_2B_9H_{11}$) leads to the formation of compounds that are a combination of the *nido*-carborane nest with the amidine fragment [20]. This promises the possibility of synthesizing complexes with simultaneous coordination of the carborane and amidine components. For our study we chose amidine 10-PrNHC(Et)=HN-7,8-$C_2B_9H_{11}$ (**1**) prepared by the nucleophilic addition of propyl amine to 10-EtC≡N-7,8-$C_2B_9H_{11}$. For the complexation reactions, we used nickel(II) phosphine complexes [$(R_2R'P)_2NiCl_2$] with ligands having different steric parameters (Tolman cone angles, θ)—$R_2R'P$ = Me_2PhP (θ = 122°), PBu_3 (θ = 132°), PPh_3 (θ = 145°) [23].

The addition of nickel(II) phosphine complexes [$(PR_2R')_2NiCl_2$] (R = R′ = Ph, Bu; R = Me, R′ = Ph) to a solution of the deprotonated amidine **1** in tetrahydrofuran at ambient temperature immediately led to a color change of the reaction mixtures color from pale yellow to dark red. Monitoring the progress of the reactions using thin layer chromatography showed that complexation occurs very quickly and is completed within 5-10 minutes. The column chromatography purification gave the corresponding π,σ-complexes [3-$R_2R'P$-3-(8-Pr*N*=C(Et)NH)-*closo*-3,1,2-$NiC_2B_9H_{10}$] (R = R′ = Ph (**2**), R = Me, R′ = Ph (**3**) and R = R′ = Bu (**4**)) in 80–83% yields (Scheme 1).

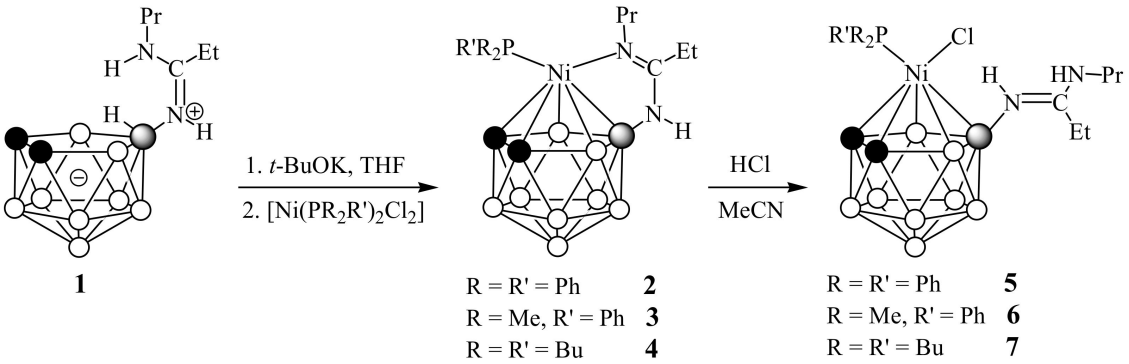

Scheme 1. Synthesis of nickelacarboranes **2**–**4** and **5**–**7**.

The initial analysis of the proposed structure of complexes **2**–**4** was carried out using standard methods of NMR and IR spectroscopy and mass spectrometry. The ^{1}H NMR spectra of complexes **2-4** demonstrated the presence of only one N*H* signal of the amidine substituent in the region of 5.04–5.53 ppm, as well as the absence of signals of the *nido*-carborane B-*H*-B bridge, suggesting that nickel was coordinated both by the pentagonal face of the carborane ligand and by one atom nitrogen of the amidine group. The pattern of the ^{11}B NMR spectra of complexes **2**–**4** is characteristic for metallacarboranes and consists of one singlet at ~4.0 ppm from the substituted boron atom and a set of four (complex **2**) or five (complexes **3** and **4**) doublets in the region from −11.2 to −27.4 ppm with total integral ratio of 1:2:3:2:1 (for **2**) and 1:2:2:1:2:1 (for **3** and **4**). The ^{1}H NMR spectra of complexes **2-4** also indicated the presence of a single phosphine ligand, while its ^{13}C NMR spectra demonstrated the characteristic splitting of signals from aromatic and/or

aliphatic groups of phosphine ligands. In the ^{31}P NMR spectra, the signals of phosphine ligands appeared at 29.3 ppm for **2**, at −2.6 ppm for **3** and at 11.9 ppm for **4**. Such chemical shifts were in good agreement with the data for similar phosphine complexes of other transitional metals [24].

In the IR spectra of complexes **2**–**4**, the NH stretching bands were observed in the region of 3447–3244 cm^{-1}, whereas the BH stretching bands appeared at ~2530 cm^{-1}. The bands corresponding to the N=C bond were at ~1635 cm^{-1} for **2** and **3**, and at 1622 cm^{-1} for **4**. The mass spectra of complexes demonstrated only peak envelopes corresponding to molecular picks of the supposed structures of complexes **2**–**4**.

The suggested structures of complexes **2**–**4** were confirmed by single crystal X-ray diffraction study on complex **2** (Figure 1).

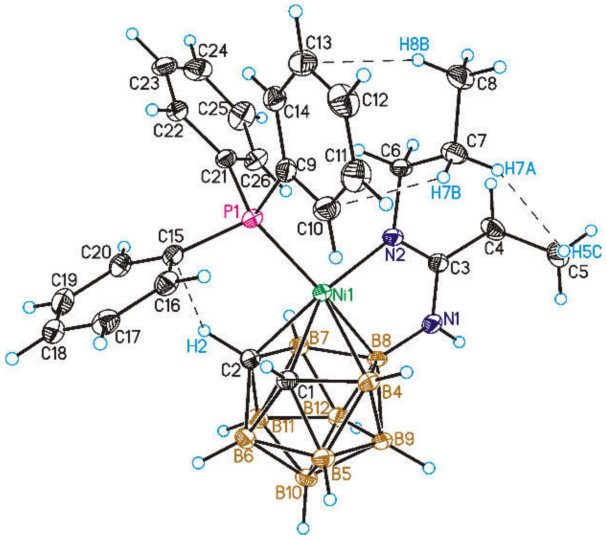

Figure 1. General view of the nickel(II) complex [3-Ph_3P-3-(8-Pr*N*=C(Et)NH)-*closo*-3,1,2-$NiC_2B_9H_{10}$] (**2**). Thermal ellipsoids are given at 50% probability level. Shortened contacts are shown by dashed lines.

The crystals of complex **2** suitable for X-ray analysis were obtained by slow evaporation from chloroform/hexane (3:1) solution. The nickel atom in the structure of **2** is approximately centered over the pentagonal face of the dicarbollide ligand with the Ni-C_2B_3 centroid distance of 1.526(2) Å. This is close to the distance found in a similar complex [3-Ph_3P-3-(8-MeOCH$_2$CH$_2$*N*=C(Et)NH)-3,1,2- $NiC_2B_9H_{10}$] (**2***) which differs only by a substituent at the N2 atom (1.533 Å) [25] and noticeably longer than in [3-Ph_3P-3-(1-Me_2NCH_2)-*closo*-3,1,2-$NiC_2B_9H_{10}$] (1.500 Å) [16], and shorter than in [3-Ph_3P-3-Cl-1-(*i*-PrNH)$_2$C-3,1,2-$NiC_2B_9H_{10}$] (1.564 Å) [26] and [3,3-$(Ph_3P)_2$-*closo*-3,1,2-$NiC_2B_9H_{11}$] (1.610 Å) [27]. The Ni-N and Ni-P bond lengths (1.914(2) and 2.2555(7) Å) are close to those found in **2*** (1.916 and 2.2532 Å) [25] and differ significantly from those found in [3-Ph_3P-3-(1-Me_2NCH_2)-*closo*-3,1,2-$NiC_2B_9H_{10}$] (2.061 and 2.166 Å, respectively) [16], reflecting the stronger electron-donating properties of the carboranylamidine ligand as compared to the carborane ligand with pendant NMe_2 group. A more detailed comparison of the structures of the complexes **2** and **2*** is presented in Table 1.

Table 1. Selected torsion angles (deg.), Ni-C_2B_3(centroid) distance and nonbonded intramolecular shortened contacts (Å) that define molecular conformation for experimental (X-ray) and calculated structure of complex **2** and comparison with **2***.

Structure Parameters	Compound 2 (X-ray)	Compound 2 *	Compound 2 (calc) *
Ni-C_2B_3(centroid)	1.526 (2)	1.533 (2)	1.545
C2-Ni1-P1-C9	143.7 (2)	128.3 (2)	125.5
C2-Ni1-P1-C15	26.3 (2)	8.3 (2)	8.0
C2-Ni1-P1-C21	−93.3 (2)	−108.9 (2)	−110.5
B8-N1-C3-C4	−179.0 (2)	−174.1 (2)	172.0
N1-C3-C4-C5	−63.2 (2)	100.0 (2)	−62.1
Ni1-N2-C6-C7	104.7 (2)	85.1 (2)	95.9
H2 . . . C15	2.66	2.54	2.45 (−2.5)
H7B . . . C10	2.76	2.75	2.74 (−1.1)
H8B . . . C13	3.04	-	2.98 (−0.7)
H5C . . . H7A	2.37	2.28 (H5C . . . H6B)	2.30 (−1.0)

* for noncovalent contacts, their attractive energies in kcal/mol are given in parenthesis.

The Ni-C_2B_3 centroid distances were only slightly different, and differences in orientation of the PPh_3 fragment were not so pronounced (within 15° of rotation about Ni-P bond). The most significant unequivalence, as expected, was observed for substituents at the N2 and C3 atoms. In spite of that, the system of shortened contacts was quite similar. One can suggest that the observed conformation can be stabilized by intramolecular noncovalent interactions. To confirm that, we carried out quantum chemical calculations of complex **2**. In optimized structure, torsion angles, which define the orientation of PPh_3 fragment, differ by ca. 18° while differences in orientation of the ethyl and propyl groups are less pronounced. Again, the system of shortened contacts, for which bond critical point were localized, was still nearly the same. Those contacts in total added −5.3 kcal/mol to the stabilization of molecular conformation. These results suggest that the variation of substituents at the N2 and C3 atoms would not significantly affect the orientation of the PPh_3 fragment relative to the carborane cage.

An attempt to obtain suitable X-ray diffraction study crystals of **3** and **4** by recrystallization from chloroform unexpectedly led to a change in the color of the solution from dark red to amaranth after ~12 h. Thin layer chromatography confirmed the formation of a new product together with the presence of small amounts of original complexes **3** and **4**. New complexes **6** and **7** were isolated by column chromatography on silica using dichloromethane as an eluent. An analysis of the NMR spectra of complexes **6** and **7** led to the assumption that the metal atom in the obtained complexes was no longer coordinated by the amidine group (Figure 2).

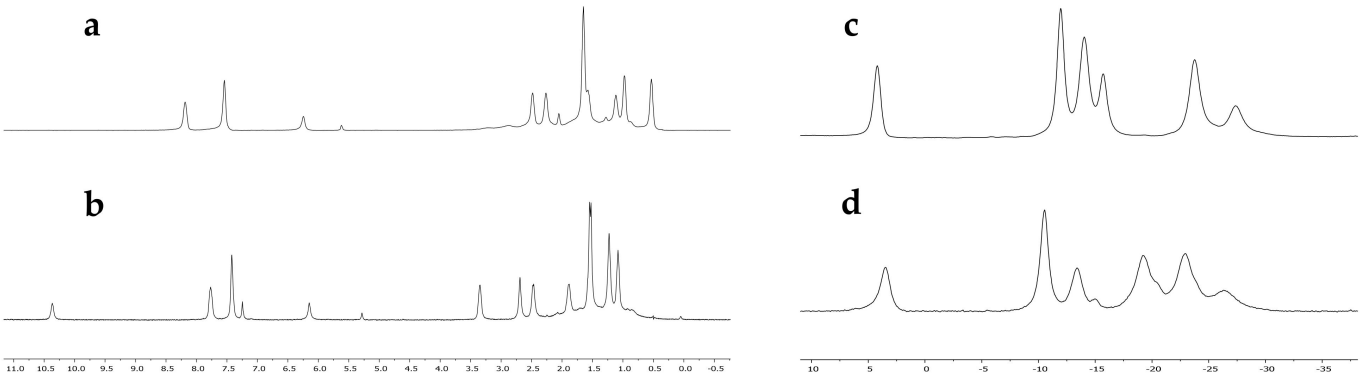

Figure 2. ^{1}H NMR spectra of complexes **3** (**a**) and **6** (**b**) and $^{11}B\{^{1}H\}$ NMR spectra of complexes **3** (**c**) and **6** (**d**).

In the ^{1}H NMR spectra of complexes **6** and **7**, signals from the second N*H* proton appeared in low field at 10.37 and 9.90 ppm for **6** and **7**, respectively (Figure 2, items a,b). This signal gave cross-pick in the ^{1}H-^{1}H COSY NMR spectrum with the methylene group of the propyl group -C***H***$_2$CH$_2$CH$_3$ (See SI). The ^{11}B NMR spectra of **6** and **7** confirmed the retention of the metallacarborane skeleton, however their spectral patterns differed from those for complexes **3** and **4** (Figure 2, items c,d). Since the newly formed complexes were neutral, we assumed that the violation of the coordination of the amidine fragment was caused by the protonation of the second nitrogen atom, and the electroneutrality of the complexes was achieved due to the coordination of the chloride ion by the nickel atom. The driving force behind this process could be the trace amounts of hydrogen chloride normally present in chloroform. To verify this assumption, we resynthesized complexes **3** and **4**, dissolved them in acetonitrile and acidified them by small amounts of concentrated hydrochloric acid (Scheme 1). This resulted in an immediate change in color of the complexes from dark red to amaranth (Figure 3). The NMR spectra confirmed the formation of complexes **6** and **7** (See SM).

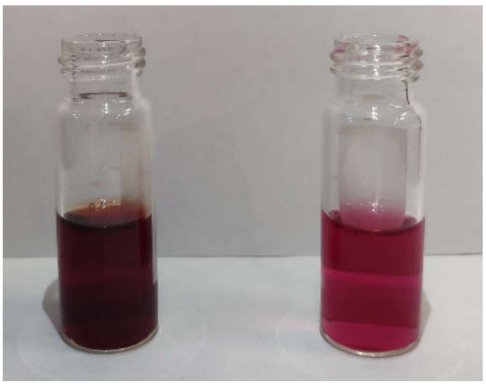

Figure 3. The color of complex **4** (left) and complex **7** (right).

For complex **2**, which did not change upon standing in chloroform solution, we carried out a similar acidification procedure with hydrochloric acid. The solution immediately changed its color from dark red to amaranth, but, unlike complexes **3** and **4**, the transformation of complex **2** into a similar complex **5** was not complete. According to the NMR spectroscopy data, the reaction mixture contained approximately 90% of complex **5** and ~10% of the original complex **2** and the addition of more amounts of hydrochloric acid did not change this ratio. An attempt to purify complex **5** by column chromatography on silica gel with dichloromethane as an eluent resulted in a mixture of complexes **2** and **5** with a new ratio of ~5:2, which can be caused by the presence of equilibrium between these complexes and the partial loss of chloride ions on the column (Scheme 2).

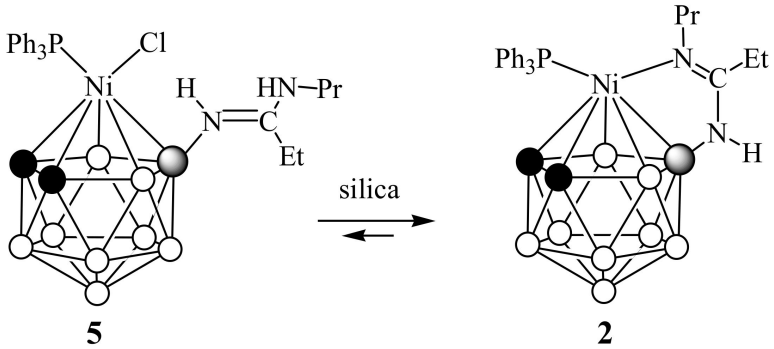

Scheme 2. Behavior of complex **5** during purification on column chromatography with silica gel.

We supposed that the less donor PPh_3 ligand made the Ni-N bond in complex **2** stronger than in complexes **3** and **4** with more donor phosphine ligands PMe_2Ph and PBu_3.

Like complexes **6** and **7**, the ^{1}H NMR spectrum of complex **5** contained the signals of two different N*H* protons: one at 9.09 ppm from the N*H*Pr group and another one at 5.53 ppm from the B-N*H*-C fragment. However, in contrast to complexes **2**–**4** in the ^{1}H NMR spectra of **5**–**7**, the signals of the CH_{carb} groups appeared in low-field at 2.57–2.80 ppm (0.44–1.12 ppm for complexes **2**–**4**). The signals of the ethyl and propyl group of the amidine substituent in **5**–**7** also underwent a number of changes and in general were shifted to the low field. For example, the signal of the methylene group of the propyl fragment -NHC$\boldsymbol{H}_2$CH$_2$CH$_3$ in complex **7** was observed at 3.41 ppm, whereas in complex **4** it appeared at 2.75 ppm. The signal of the methylene group of the ethyl substituent was located at 2.54 ppm for **7** in contrast with 2.22 ppm for **4**. At the same time, the signals of the carbon atom of the methylene group of the propyl fragment -NH$\boldsymbol{C}$H$_2$CH$_2$CH$_3$ in ^{13}C NMR spectra of **5**–**7** underwent the high field shift from ~55 ppm for **2**–**4** to ~46 ppm, whereas the signal of the methylene group of the ethyl fragment demonstrated a slight high field shift from ~23–24 ppm for **2**–**4** to ~26–30 ppm for **5**–**7**. In the ^{11}B NMR spectra of complexes **5**–**7**, the singlet from the substituted boron atom was observed at 1.9 ppm for **5** and at 3.5 ppm for **6** and **7**. Other signals appeared as groups of four (complex **5**) or five (complexes **6** and **7**) doublets in the region from −10.2 to −26.3 ppm with the total integral ratios 1:2:1:4:1 for **5** and 1:2:1:2:2:1 for **6** and **7**. The chemical shifts of phosphine ligands in the ^{31}P NMR spectra of **5**–**7** were close to those for **2**–**4**. In the IR spectra of **5**–**7**, the NH and BH stretching bands were observed in the region of 3402–3223 cm^{-1} and ~2555 cm^{-1}, respectively, whereas the bands corresponding to the N=C bond appeared at 1632, 1626 and 1630 cm^{-1} for **5**, **6** and **7**, respectively. The mass spectra of complexes **5**–**7** performed using the MS MALDI technique contained two main sets of signals corresponding to the molecular picks of complexes **5**–**7** themselves and complexed with the loss of the chloride ligand. For example, the MALDI mass spectrum of complex **6** contained a typical carborane envelope centered at m/z 477.253 corresponding to the molecular ion pick and another one centered at m/z 442.275, that corresponded to the loss of the chloride ligand by complex **6**.

3. Conclusions

In this work the utility of using the *nido*-carboranyl amidine 10-PrNHC(Et)=HN-7,8-$C_2B_9H_{11}$ in the complexation reactions with different nickel(II) phosphine complexes was demonstrated. As a result, a series of novel half-sandwich nickel(II) π,σ-complexes [3-R$_2$R′P-3-(8-Pr*N*=C(Et)NH)-*closo*-3,1,2-Ni$C_2B_9H_{10}$] (R = R′ = Ph, Bu; R = Me, R′ = Ph) was prepared. The crystal molecular structure of [3-Ph_3P-3- (8-Pr*N*=C(Et)NH)-*closo*-3,1,2-Ni$C_2B_9H_{10}$] was determined by single crystal X-ray diffraction. The acidification of obtained complexes with HCl led to the breaking of the Ni-N bond with the formation of the corresponding nickel(II) π-complexes [3-Cl-3-R′R$_2$P- 8-PrNH=C(Et)NH-*closo*-3,1,2-Ni$C_2B_9H_{10}$] (R = R′ = Ph, Bu; R = Me, R′ = Ph). The process was accompanied by a change in the color of complexes from dark red to amaranth one. In this regard, the obtained complexes can be considered as potential acid-base indicators.

4. Experimental Section

4.1. Reagents and Methods

The amidine 10-PrNHC(Et)=HN-7,8-$C_2B_9H_{11}$ (**1**) was prepared according to procedure from the literature [20]. Dichlorobis(triphenylphosphine)nickel(II), dichlorobis (dimethylphenylphosphine)nickel(II) and dichlorobis(tributylphosphine)nickel(II) were synthesized according to the previously described methods [28]. Tetrahydrofuran was dried using standard procedure [29]. All manipulations were carried out in air. The reaction progress was monitored by thin-layer chromatography (Merck F254 silica gel on aluminum plates) and visualized using 0.5% $PdCl_2$ in 1% HCl in aq. MeOH (1:10). Acros Organics silica gel (0.060–0.200 mm) was used for column chromatography. The NMR spectra at 400.1 MHz (^{1}H), 128.4 MHz (^{11}B), 100.0 MHz (^{13}C) and 162 MHz (^{31}P)

were recorded with a Varian Inova 400 spectrometer. The residual signal of the NMR solvent relative to tetramethylsilane was taken as an internal reference for ^{1}H and ^{13}C NMR spectra. ^{11}B NMR spectra were referenced using $BF_3{\cdot}Et_2O$ as an external standard. ^{31}P NMR spectra were cited relative to 85% H_3PO_4 as an external standard. Infrared spectra were recorded on an IR Prestige-21 (SHIMADZU, Kyoto, Japan) instrument. UV/Vis spectra in chloroform were recorded with a SF-2000 spectrophotometer (OKB SPECTR LLC, Saint-Petersburg, Russia) using 1 cm cuvettes. MALDI mass spectra (positive ion mode) were acquired using a Bruker AutoFlex II reflector time-of-flight device equipped with an N_2 laser (337 nm, 2.5 ns pulse). *Trans*-2-[3-(4-*tert*-butylphenyl)-2-methyl-2-propenylidene]malononitrile (DCTB, ≥98%, Sigma-Aldrich, Louis, MO, USA) was chosen as a matrix, matrix-to-analyte molar ratio in spotted probes being more than 1000/1. High resolution mass spectra (HRMS) were measured on a Bruker micrOTOF II instrument using electrospray ionization (ESI). The measurements were done in a positive ion mode with mass range from *m*/*z* 50 to *m*/*z* 3000.

*4.2. Synthesis of [3-Ph$_3$P-3-(8-PrN=C(Et)NH)-closo-3,1,2-NiC$_2$B$_9$H$_{10}$] (**2**)*

The potassium *tert*-butoxide (0.34 g, 3.00 mmol) was added to a solution of **1** (0.15 g, 0.60 mmol) in dry tetrahydrofuran (15 mL). The mixture was stirred for ~10 min at room temperature and [Ni(PPh$_3$)$_2$Cl$_2$] (0.47 g, 0.72 mmol) was added by one portion. The pale-yellow color of the reaction mixture was immediately turned to dark red. The reaction mixture was stirred at room temperature in air for about 30 min and the solvent was evaporated under reduced pressure. The residue was treated with CH_2Cl_2 (20 mL) and water (20 mL). The insoluble particles were filtered off and the organic layer was separated, washed with water (2 × 20 mL) and evaporated under reduced pressure. The column chromatography on silica gel was used for the purification of the substance with hexane:CH_2Cl_2 (2:1) as an eluent to give maroon solid of **2** (0.28 g, 83% yield). The crystals suitable for X-ray analysis were obtained by slow evaporation from chloroform/hexane (3:1) solution.

^{1}H NMR ($CDCl_3$, ppm): δ 7.82 (6H, Ph), 7.44 (9H, Ph), 5.09 (1H, N*H*), 2.27 (2H, NHCH_2CH$_2$CH$_3$), 2.14 (2H, CH_2CH$_3$), 1.25 (2H, NHCH$_2$CH_2CH$_3$), 1.09 (3H, CH$_2$CH_3), 0.44 (2H, s, CH_{carb}), 0.04 (3H, NHCH$_2$CH$_2$CH_3), 3.4–0.2 (8H, br s, B*H*). ^{13}C NMR ($CDCl_3$, ppm): δ 176.9 (NH=*C*), 134.0 (*o*-Ph, d, *J* = 12 Hz), 131.2 (Ph, d, *J* = 37 Hz), 130.8 (*p*-Ph), 128.9 (*m*-Ph, d, *J* = 9 Hz), 56.1 (NHCH$_2$CH$_2$CH$_3$), 25.1 (NHCH$_2$CH$_2$CH$_3$), 24.0 (CH$_2$), 17.2 (*C*H$_{carb}$), 11.9 (*C*H$_3$), 10.4 (NHCH$_2$CH$_2$CH$_3$). ^{31}P NMR ($CDCl_3$, ppm): 29.3 (s, *P*Ph$_3$). ^{11}B NMR ($CDCl_3$, ppm): δ 4.0 (1B, s), −11.2 (2B, d), −13.6 (3B, d), −23.5 (2B, d), −26.7 (1B, d). IR (film, cm^{-1}): 3437 (ν_{N-H}), 3411 (ν_{N-H}), 3308, 3245, 3057, 2966 (ν_{C-H}), 2933 (ν_{C-H}), 2875 (ν_{C-H}), 2551 (br, ν_{B-H}), 1635 ($\nu_{N=C}$), 1557, 1503, 1480, 1436, 1380, 1325, 1310. UV/VIS (ʎ, nm): 248, 330, 510. MALDI MS: *m*/*z* for $C_{26}H_{38}B_9N_2NiP$: calcd 565.299 [M]$^+$, obsd 565.288 [M]$^+$ (100).

*4.3. Synthesis of [3-PhMe$_2$P-3-(8-PrN=C(Et)NH)-closo-3,1,2-NiC$_2$B$_9$H$_{10}$] (**3**)*

The procedure was analogous to the preparation of **2** using **1** (0.13 g, 0.52 mmol), potassium *tert*-butoxide (0.30 g, 2.60 mmol) and [Ni(PMe$_2$Ph)$_2$Cl$_2$] (0.25 g, 0.62 mmol) in dry tetrahydrofuran (15 mL). The column chromatography on silica gel was used for the purification of the substance with CH_2Cl_2 as an eluent to give maroon solid of **3** (0.19 g, 82% yield).

^{1}H NMR (acetone-d$_6$, ppm): δ 8.19 (2H, Ph), 7.54 (3H, Ph), 6.25 (1H, N*H*), 2.48 (2H, NHCH_2CH$_2$CH$_3$), 2.26 (2H, CH_2CH$_3$), 1.65 (6H, P(CH_3)$_2$), 1.57 (2H, NHCH$_2$CH_2CH$_3$), 1.12 (2H, s, CH_{carb}), 0.98 (3H, CH$_2$CH_3), 0.53 (3H, NHCH$_2$CH$_2$CH_3), 3.4–0.4 (8H, br s, B*H*). ^{13}C NMR (acetone-d$_6$, ppm): δ 177.7 (NH=*C*), 131.3 (Ph, d, *J* = 18 Hz), 131.2 (*o*-Ph, d, *J* = 12 Hz), 130.3 (*p*-Ph), 128.8 (*m*-Ph, d, *J* = 10 Hz), 54.3 (NHCH$_2$CH$_2$CH$_3$), 26.5 (NHCH$_2$CH$_2$CH$_3$), 23.4 (CH$_2$), 14.7 (CH$_{carb}$), 13.7 (P(CH$_3$)$_2$, d, *J* = 24 Hz), 11.7 (CH$_3$), 10.3 (NHCH$_2$CH$_2$CH$_3$). ^{31}P NMR (acetone-d$_6$, ppm): −2.6 (s, *P*Me$_2$Ph). ^{11}B NMR (acetone-d$_6$, ppm): δ 4.2 (1B, s), −12.0 (2B, d, *J* = 137 Hz), −14.0 (2B, d, *J* = 156 Hz), −15.7 (1B, d, *J* = 147 Hz), −23.8 (2B, d, *J* = 143 Hz), −27.4 (1B, d, *J* = 144 Hz). IR (film, cm^{-1}): 3410 (ν_{N-H}), 3244 (ν_{N-H}), 2962

($\nu_{C\text{-}H}$), 2930 ($\nu_{C\text{-}H}$), 2874 ($\nu_{C\text{-}H}$), 2525 (br, $\nu_{B\text{-}H}$), 1636 ($\nu_{N=C}$), 1568, 1493, 1437, 1377, 1300, 1292. ESI HRMS: *m*/*z* for $C_{16}H_{34}B_9N_2NiP$: calcd 441.2696 $[M]^+$, obsd 441.2696 $[M]^+$ (100).

*4.4. Synthesis of [3-Bu$_3$P-3-(8-PrN=C(Et)NH)-closo-3,1,2-NiC$_2$B$_9$H$_{10}$] (**4**)*

The procedure was analogous to the preparation of **2** using **1** (0.16 g, 0.64 mmol), potassium *tert*-butoxide (0.36 g, 3.20 mmol) and $[Ni(PBu_3)_2Cl_2]$ (0.26 g, 0.77 mmol) in dry tetrahydrofuran (15 mL). The column chromatography on silica gel was used for the purification of the substance with CH_2Cl_2 as an eluent to give maroon solid of **3** (0.25 g, 80% yield).

^{1}H NMR ($CDCl_3$, ppm): δ 5.04 (1H, N*H*), 2.75 (2H, NHCH_2CH$_2$CH$_3$), 2.22 (2H, CH_2CH$_3$), 1.70 (2H, NHCH$_2$CH_2CH$_3$), 1.61 (6H, P(CH_2CH$_2$CH$_2$CH$_3$)$_3$), 1.50 (6H, P(CH$_2$CH$_2$CH_2CH$_3$)$_3$), 1.40 (6H, P(CH$_2$CH_2CH$_2$CH$_3$)$_3$), 1.06 (3H, CH$_2$CH_3), 0.93 (14H, NHCH$_2$CH$_2$CH_3 + P(CH$_2$CH$_2$CH$_2$CH_3)$_3$ + CH_{carb}), 3.4–0.2 (8H, br s, B*H*). ^{13}C NMR ($CDCl_3$, ppm): δ 176.6 (NH=*C*), 55.2 (NHCH_2CH$_2$CH$_3$), 26.7 (NHCH$_2$CH_2CH$_3$), 26.5 (P(CH_2CH$_2$CH$_2$CH$_3$)$_3$, d, *J* = 50 Hz), 24.4 (P(CH$_2$CH_2CH$_2$CH$_3$)$_3$, d, *J* = 12 Hz), 24.2 (*C*H$_2$), 23.5 (P(CH$_2$CH_2CH$_2$CH$_3$)$_3$, d, *J* = 20 Hz), 14.0 (*C*H$_{carb}$), 13.7 (P(CH$_2$CH$_2$CH_2CH$_3$)$_3$), 11.8 (*C*H$_3$), 11.5 (NHCH$_2$CH$_2$*C*H$_3$). ^{31}P NMR ($CDCl_3$, ppm): 11.9 (s, *P*Bu$_3$). ^{11}B NMR ($CDCl_3$, ppm): δ 3.8 (1B, s), −11.8 (2B, d), −14.3 (2B, d), −15.1 (1B, d), −23.6 (2B, d), −26.8 (1B, d). IR (film, cm^{-1}): 3447 ($\nu_{N\text{-}H}$), 3408 ($\nu_{N\text{-}H}$), 2957 ($\nu_{C\text{-}H}$), 2932 ($\nu_{C\text{-}H}$), 2872 ($\nu_{C\text{-}H}$), 2544 (br, $\nu_{B\text{-}H}$), 1622 ($\nu_{N=C}$), 1557, 1497, 1464, 1379, 1283. MALDI MS: *m*/*z* for $C_{20}H_{50}B_9N_2NiP$: calcd 506.402 $[M+H]^+$, obsd 506.400 $[M+H]^+$ (100).

*4.5. General Procedure for the Synthesis of [3-Cl-3-R'R$_2$P-8-PrN=C(Et)NH-closo-3,1,2-NiC$_2$B$_9$H$_{10}$] (**5**–**7**)*

To the *N*-coordinated complexes **2**–**4** (0.40 mmol) dissolved in MeCN (10 mL), one drop (~0.1 mL) of concentrated HCl was added at room temperature. The dark red color of solution was immediately changed to amaranth. The solution was stirred for 5 min and evaporated under reduced pressure to give amaranth solid of **5**–**7.** In the case of complexes **6** and **7**, the column chromatography on silica gel was used for the purification with CH_2Cl_2 as an eluent.

Spectral data for [3-Cl-3-Ph$_3$P-8-Pr*N*=C(Et)NH-*closo*-3,1,2-NiC$_2$B$_9$H$_{10}$] (**5**)

Yield 0.18 g (75%).

^{1}H NMR ($CDCl_3$, ppm): δ 9.09 (1H, N*H*Pr), 7.62 (6H, Ph), 7.31 (9H, Ph), 5.53 (1H, N*H*), 3.22 (2H, NHCH_2CH$_2$CH$_3$), 2.57 (2H, CH_{carb}), 1.86 (4H, NHCH$_2$CH_2CH$_3$ + CH_2CH$_3$), 0.93 (6H, NHCH$_2$CH$_2$CH_3 + CH$_2$CH_3), 3.8–0.3 (8H, br s, B*H*). ^{13}C NMR ($CDCl_3$, ppm): δ 167.5 (NH=*C*), 134.3 (Ph), 133.7 (Ph), 130.4 (Ph), 128.2 (Ph), 45.6 (NHCH_2CH$_2$CH$_3$), 30.8 (*C*H$_2$), 25.2 (NHCH$_2$CH_2CH$_3$), 23.2 (*C*H$_{carb}$), 11.1 (*C*H$_3$), 9.8 (NHCH$_2$CH$_2$*C*H$_3$). ^{31}P NMR ($CDCl_3$, ppm): 28.2 (s, *P*Ph$_3$). ^{11}B NMR ($CDCl_3$, ppm): δ 1.9 (1B, s), −10.2 (2B, d), −12.3 (1B, d), −20.8 (4B, d), −24.2 (1B, d). IR (film, cm^{-1}): 3397 ($\nu_{N\text{-}H}$), 3302 ($\nu_{N\text{-}H}$), 3233 ($\nu_{N\text{-}H}$), 3059, 2966 ($\nu_{C\text{-}H}$), 2967 ($\nu_{C\text{-}H}$), 2928 ($\nu_{C\text{-}H}$), 2878 ($\nu_{C\text{-}H}$), 2560 (br, $\nu_{B\text{-}H}$), 1632 ($\nu_{N=C}$), 1553, 1501, 1481, 1437, 1385, 1259. UV/VIS (ʎ, nm): 280, 302, 486. MALDI MS: *m*/*z* for $C_{26}H_{39}B_9N_2ClNiP$: calcd 601.277 $[M]^+$, obsd 601.293 $[M]^+$ (10), *m*/*z* for $C_{26}H_{39}B_9N_2NiP$: calcd 566.308 $[M\text{-}Cl]^+$, obsd 566.321 $[M\text{-}Cl]^+$ (90).

Spectral data for [3-Cl-3-PhMe$_2$P-8-Pr*N*=C(Et)NH-*closo*-3,1,2-NiC$_2$B$_9$H$_{10}$] (**6**)

Yield 0.16 g (84%).

^{1}H NMR (acetone-d$_6$, ppm): δ 10.37 (1H, N*H*Pr), 7.77 (2H, Ph), 7.42 (3H, Ph), 6.15 (1H, N*H*), 3.35 (2H, NHCH_2CH$_2$CH$_3$), 2.69 (2H, s, CH_{carb}), 2.48 (2H, CH_2CH$_3$), 1.89 (2H, NHCH$_2$CH_2CH$_3$), 1.53 (6H, P(CH_3)$_2$), 1.23 (3H, CH$_2$CH_3), 1.08 (3H, NHCH$_2$CH$_2$CH_3), 3.0–0.5 (8H, br s, B*H*). ^{13}C NMR (acetone-d$_6$, ppm): δ 130.2 (Ph), 130.0 (Ph), 129.0 (Ph), 46.1 (NHCH_2CH$_2$CH$_3$), 26.2 (*C*H$_2$), 23.4 (NHCH$_2$CH_2CH$_3$), 14.8 (P(*C*H$_3$)$_2$), 11.7 (NHCH$_2$CH$_2$*C*H$_3$), 9.7 (*C*H$_3$). ^{31}P NMR (acetone-d$_6$, ppm): −2.53 (s, *P*Me$_2$Ph). ^{11}B NMR (acetone-d$_6$, ppm): δ 3.5 (1B, s), −10.5 (2B, d, *J* = 133 Hz), −13.4 (1B, d, *J* = 145 Hz), −19.2 (2B, d, *J* = 140 Hz), −22.9 (2B, d, *J* = 117 Hz), −26.3 (1B, d, *J* = 172 Hz). IR (film, cm^{-1}): 3402 ($\nu_{N\text{-}H}$), 3259 ($\nu_{N\text{-}H}$), 3227 ($\nu_{N\text{-}H}$), 3053, 2968 ($\nu_{C\text{-}H}$), 2934 ($\nu_{C\text{-}H}$), 2878 ($\nu_{C\text{-}H}$), 2548 (br, $\nu_{B\text{-}H}$), 1626 ($\nu_{N=C}$), 1557, 1435, 1421, 1384, 1361, 1296. MALDI MS: *m/z* for $C_{16}H_{35}B_9N_2ClNiP$: calcd 477.245

$[M]^+$, obsd 477.253 $[M]^+$ (23), *m*/*z* for $C_{16}H_{35}B_9N_2NiP$: calcd 442.276 $[M\text{-}Cl]^+$, obsd 442.275 $[M\text{-}Cl]^+$ (77).

Spectral data for [3-Cl-3-Bu_3P-8-Pr*N*=C(Et)NH-*closo*-3,1,2-$NiC_2B_9H_{10}$] (**7**)

Yield 0.19 g (88%).

^{1}H NMR ($CDCl_3$, ppm): δ 9.90 (1H, N*H*Pr), 6.22 (1H, N*H*), 3.41 (2H, q, J = 7.5 Hz, $NHCH_2CH_2CH_3$), 2.80 (2H, s, CH_{carb}), 2.54 (2H, q, J = 7.6 Hz, CH_2CH_3), 1.90 (2H, m, J = 7.5 Hz, $NHCH_2CH_2CH_3$), 1.58 (12H, $P(CH_2CH_2CH_2CH_3)_3$), 1.39 (6H, $P(CH_2CH_2CH_2CH_3)_3$), 1.28 (3H, t, J = 7.6 Hz, CH_2CH_3), 1.07 (3H, t, J = 7.5 Hz, $NHCH_2CH_2CH_3$), 0.93 (9H, $P(CH_2CH_2CH_2CH_3)_3$), 3.3–0.9 (8H, br s, B*H*). ^{13}C NMR ($CDCl_3$, ppm): δ 46.2 ($NHCH_2CH_2CH_3$), 30.8 (CH_{carb}), 26.3 (CH_2), 26.2 ($P(CH_2CH_2CH_2CH_3)_3$), 24.5 ($P(CH_2CH_2CH_2CH_3)_3$), 23.7 ($P(CH_2CH_2CH_2CH_3)_3$, 23.6 ($NHCH_2CH_2CH_3$), 11.6 ($NHCH_2CH_2CH_3$), 10.3 (CH_3), 13.8 ($P(CH_2CH_2CH_2CH_3)_3$). ^{31}P NMR ($CDCl_3$, ppm): 11.7 (s, *P*Bu_3). ^{11}B NMR ($CDCl_3$, ppm): δ 3.5 (1B, s), −10.6 (2B, d, J = 127 Hz), −13.9 (1B, d, J = 129 Hz), −20.3 (2B, d, J = 135 Hz), −23.7 (2B, d), −26.3 (1B, d). IR (film, cm^{-1}): 3223 ($\nu_{N\text{-}H}$), 2957 ($\nu_{C\text{-}H}$), 2930 ($\nu_{C\text{-}H}$), 2872 ($\nu_{C\text{-}H}$), 2550 (br, $\nu_{B\text{-}H}$), 1630 ($\nu_{N=C}$), 1552, 1462, 1415, 1379, 1342, 1300. UV/VIS (ʎ, nm): 246, 324, 517. MALDI MS: *m*/*z* for $C_{20}H_{51}B_9N_2ClNiP$: calcd 541.371 $[M]^+$, obsd 541.373 $[M]^+$ (9) *m*/*z* for $C_{20}H_{51}B_9N_2NiP$: calcd 506.402 $[M\text{-}Cl]^+$, obsd 506.443 $[M\text{-}Cl]^+$ (91).

4.6. Single Crystal X-ray Diffraction Study

X-ray experiment for compound **2** was carried out using a SMART APEX2 CCD diffractometer (λ(Mo-Kα) = 0.71073 Å, graphite monochromator, ω-scans) at 120 K. Collected data were processed by the SAINT and SADABS programs incorporated into the APEX2 program package [30]. The structure was solved by direct methods and refined by the full-matrix least-squares procedure against F^2 in anisotropic approximation. The refinement was carried out with the SHELXTL program [31]. The CCDC number 2065468 contains the supplementary crystallographic data (Supplementary Materials) for this paper. These data can be obtained free of charge via www.ccdc.cam.ac.uk/data_request/cif (accessed on 19 March 2021).

Crystallographic data for **2***:* $C_{26}H_{38}B_9NiN_2P{\cdot}CHCl_3$ are triclinic, space group *P*-1: a = 10.0074(6) Å, b = 11.0974(6) Å, c = 16.8683(8) Å, α = 76.8900(10)°, β = 81.3380(10)°, γ = 67.4720(10)°, V = 1681.05(16) Å^3, Z = 2, M = 684.92, d_{cryst} = 1.353 g·cm^{-3}. $wR2$= 0.1312 calculated on F^2_{hkl} for all 8953 independent reflections with $2\theta < 58.3°$, (GOF = 1.048, R = 0.0528 calculated on F_{hkl} for 6268 reflections with $I > 2\sigma(I)$).

4.7. Quantum Chemical Calculation

Optimization of the geometry of compound **2** was carried out using the Gaussian program [32] at PBE0/def2tzvp level of approximation, which was adopted in our earlier calculations [33–36]. The AIM theory [37,38] was utilized to search for bond critical points of molecular electron density. Correlation of interatomic energy and potential energy density at bond critical point (E=1/2V(r)) [39,40] was adopted for estimation of the energy of noncovalent intramolecular interactions taking into account its reliability for energetic analysis [41–43].

Supplementary Materials: The following are available online at https://www.mdpi.com/2073-4352/11/3/306/s1. Figure S1–S29 NMR spectra of compounds **2**–**7**.

Author Contributions: Synthesis and writing, NMR, IR research analysis, M.Y.S.; synthesis, S.A.E.; X-ray diffraction study, K.Y.S.; supervision, writing, I.B.S.; editing V.I.B. All authors have read and agreed to the published version of the manuscript.

Funding: This work was supported by the Russian Science Foundation (№ 19-73-00229).

Institutional Review Board Statement: Not applicable.

Informed Consent Statement: Not applicable.

Data Availability Statement: The data presented in this study are available in Supplementary Materials.

Acknowledgments: The NMR spectroscopy and X-ray diffraction experiments were performed using equipment of the Center for Molecular Structure Studies at A.N. Nesmeyanov Institute of Organoelement Compounds, operating with financial support of the Ministry of Science and Higher Education of the Russian Federation. The authors thank Vitaliy Yu. Markov (M.V. Lomonosov Moscow State University) for collecting MALDI mass spectra.

Conflicts of Interest: The authors declare no conflict of interest.

References

1. Grimes, R.N. Transitional metal metallacarbaboranes. In *Comprehensive Organometallic Chemistry II*; Elsevier: Oxford, UK, 1995; Volume 1, pp. 373–430.
2. Grimes, R.N. Metallacarboranes in the new millennium. *Coord. Chem. Rev.* **2000**, *200*, 773–811. [CrossRef]
3. Hosmane, N.S.; Maguire, J.A. Metallacarboranes of *d*- and *f*-block metals. In *Comprehensive Organometallic Chemistry III*; Elsevier: Oxford, UK, 2007; Volume 3, pp. 175–264.
4. Bregadze, V.I. Dicarba-*closo*-dodecaboranes $C_2B_{10}H_{12}$ and their derivatives. *Chem. Rev.* **1992**, *92*, 209–223. [CrossRef]
5. Yinghuai, Z.; Yulin, Z.; Carpenter, K.; Maguire, J.A.; Hosmane, N.S. Synthesis and catalytic activities of Group 4 metal complexes derived from $C_{(cage)}$-appended cyclohexyloxocarborane trianion. *J. Organomet. Chem.* **2005**, *690*, 2802–2808. [CrossRef]
6. Yinghuai, Z.; Lo Pei Sia, S.; Kooli, F.; Carpenter, K.; Kemp, R.A. Another example of carborane based trianionic ligand: Syntheses and catalytic activities of cyclohexylamino tailed ortho-carboranyl zirconium and titanium dicarbollides. *J. Organomet. Chem.* **2005**, *690*, 6284–6291. [CrossRef]
7. Shen, H.; Chan, H.-S.; Xie, Z. Guanylation of amines catalyzed by a half-sandwich titanacarborane amide complex. *Organometallics* **2006**, *25*, 5515–5517. [CrossRef]
8. Gao, M.; Tang, Y.; Xie, M.; Qian, C.; Xie, Z. Synthesis, structure, and olefin polymerization behavior of constrained-geometry Group 4 metallacarboranes incorporating imido-dicarbollyl ligands. *Organometallics* **2006**, *25*, 2578–2584. [CrossRef]
9. Shen, H.; Xie, Z. Titanacarborane Amide catalyzed transamination of guanidines. *Organometallics* **2008**, *27*, 2685–2687. [CrossRef]
10. Yinghuai, Z.; Hosmane, N.S. Carborane-based transitional metal complexes and their catalytic application for olefin polymerization: Current and future perspectives. *J. Organomet. Chem.* **2013**, *747*, 25–29. [CrossRef]
11. Sivaev, I.B. Ferrocene and transition metal bis(dicarbollides) as platform for design of rotatory molecular switches. *Molecules* **2017**, *22*, 2201. [CrossRef]
12. Anufriev, S.A.; Timofeev, S.V.; Anisimov, A.A.; Suponitsky, K.Y.; Sivaev, I.B. bis(dicarbollide) complexes of transition metals as a platform for molecular switches. Study of complexation of 8,8′-bis(methylsulfanyl) derivatives of cobalt and iron bis(dicarbollides). *Molecules* **2020**, *25*, 5745. [CrossRef] [PubMed]
13. Shen, H.; Chan, H.-S.; Xie, Z. Synthesis, structure, and reactivity of $[\sigma{:}\eta^1{:}\eta^5\text{-}(OCH_2)(Me_2NCH_2)C_2B_9H_9]Ti(NR_2)$ (R = Me, Et). *Organometallics* **2007**, *26*, 2694–2704. [CrossRef]
14. Lee, J.-D.; Lee, Y.-J.; Son, K.-C.; Han, W.-S.; Cheong, M.; Ko, J.; Kang, S.O. Synthesis, characterization, and reactivity of new types of constrained geometry Group 4 metal complexes derived from picolyl-substituted dicarbollide ligand systems. *J. Organomet. Chem.* **2007**, *692*, 5403–5413. [CrossRef]
15. Anufriev, S.A.; Sivaev, I.B.; Nakamura, H. Two possible ways to combine boron and gadolinium for Gd-quided BNCT. A concept. *Phosphorus Sulfur Silicon Relat. Elem.* **2020**, *195*, 910–917. [CrossRef]
16. Park, J.-S.; Kim, D.-H.; Kim, S.-J.; Ko, J.; Kim, S.H.; Cho, S.; Lee, C.-H.; Kang, S.O. Preparation and reactions of a half-sandwich dicarbollyl nickel(II) complexes containing a dimethylamino pendent group. *Organometallics* **2001**, *20*, 4483–4491. [CrossRef]
17. Park, J.-S.; Kim, D.-H.; Ko, J.; Kim, S.H.; Cho, S.; Lee, C.-H.; Kang, S.O. Half-sandwich iron(II) and ruthenium(II) complexes with the dicarbollylamino ligand system. *Organometallics* **2001**, *20*, 4632–4640. [CrossRef]
18. Kim, D.-H.; Won, J.H.; Kim, S.-J.; Ko, J.; Kim, S.H.; Cho, S.; Kang, S.O. Dicarbollide analogues of the constrained-geometry polymerization catalyst. *Organometallics* **2001**, *20*, 4298–4300. [CrossRef]
19. Lee, J.-D.; Lee, Y.-J.; Son, K.-C.; Cheong, M.; Ko, J.; Kang, S.O. New types of constrained geometry Group 4 metal complexes derived from the aminomethyldicarbollyl ligand system: Synthesis and structural characterization of mono-dicarbollylamino and bis-dicarbollylamino Group 4 metal complexes. *Organometallics* **2007**, *26*, 3374–3384. [CrossRef]
20. Stogniy, M.Y.; Erokhina, S.A.; Suponitsky, K.Y.; Anisimov, A.A.; Godovikov, I.A.; Sivaev, I.B.; Bregadze, V.I. Synthesis of novel carboranyl amidines. *J. Organomet. Chem.* **2020**, *909*, 121111. [CrossRef]
21. Stogniy, M.Y.; Erokhina, S.A.; Suponitsky, K.Y.; Anisimov, A.A.; Sivaev, I.B.; Bregadze, V.I. Nucleophilic addition reactions to the ethylnitrilium derivative of *nido*-carborane 10-EtC≡N-7,8-$C_2B_9H_{11}$. *New J. Chem.* **2018**, *42*, 17958–17967. [CrossRef]
22. Stogniy, M.Y.; Erokhina, S.A.; Anisimov, A.A.; Suponitsky, K.Y.; Sivaev, I.B.; Bregadze, V.I. 10-$NCCH_2CH_2OCH_2CH_2C{\equiv}N$-7,8-$C_2B_9H_{11}$: Synthesis and reactions with various nucleophiles. *Polyhedron* **2019**, *174*, 114170. [CrossRef]
23. Clavier, H.; Nolan, S.P. Percent buried volume for phosphine and *N*-heterocyclic carbene ligands: Steric properties in organometallic chemistry. *Chem. Commun.* **2010**, *46*, 841–861. [CrossRef]
24. Hunter, A.D.; Williams, T.R.; Zarzyczny, B.M.; Bottesch, H.W.; Dolan, S.A.; McDowell, K.A.; Thomas, D.N.; Mahler, C.H. Correlations among ^{31}P NMR coordination chemical shifts, Ru–P bond distances, and enthalpies of reaction in $Cp'Ru(PR_3)_2Cl$ complexes (Cp' = η^5-C_5H_5, η^5-C_5Me_5; PR_3 = PMe_3, $PPhMe_2$, PPh_2Me, PPh_3, PEt_3, P^nBu_3). *Organometallics* **2016**, *35*, 2701–2706. [CrossRef]

25. Stogniy, M.Y.; Erokhina, S.A.; Suponitsky, K.Y.; Markov, V.Y.; Sivaev, I.B. Synthesis and crystal structures of nickel(II) and palladium(II) complexes with *o*-carboranyl amidine ligands. *Dalton Trans.* **2021**, *50*. [CrossRef]
26. Yao, Z.-J.; Jin, G.-X. Synthesis, reactivity, and structural transformation of mono- and binuclear carboranylamidinate-based 3d metal complexes and metallacarborane derivatives. *Organometallics* **2012**, *31*, 1767–1774. [CrossRef]
27. Erdman, A.A.; Zubreichuk, Z.P.; Knizhnikov, V.A.; Maier, A.A.; Aleksandrov, G.G.; Nefedov, S.E.; Eremenko, I.L. Synthesis and the structure of the triphenylphosphine complex of *o*-nickelacarborane, 3,3-$(PPh_3)_2$-3,1,2-$NiC_2B_9H_{11}$. *Russ. Chem. Bull.* **2001**, *50*, 2248–2250. [CrossRef]
28. Standley, E.A.; Smith, S.J.; Müller, P.; Jamison, T.F. A broadly applicable strategy for entry into homogeneous nickel(0) catalysts from air-stable nickel(II) complexes. *Organometallics* **2014**, *33*, 2012–2018. [CrossRef] [PubMed]
29. Armarego, W.L.F.; Chai, C.L.L. *Purification of Laboratory Chemicals*; Butterworth-Heinemann: Burlington, MA, USA, 2009.
30. Bruker. *APEX2 and SAINT*; Bruker AXS Inc.: Madison, WI, USA, 2014.
31. Sheldrick, G.M. Crystal structure refinement with SHELXL. *Acta Cryst. C* **2015**, *71*, 3–8. [CrossRef] [PubMed]
32. Frisch, M.J.; Trucks, G.W.; Schlegel, H.B.; Scuseria, G.E.; Robb, M.A.; Cheeseman, J.R.; Montgomery, J.A.; Kudin, K.N., Jr.; Burant, J.C.; Millam, J.M.; et al. *Gaussian 03, Revision E.01*; Gaussian Inc.: Wallingford, CT, USA, 2004.
33. Anufriev, S.A.; Sivaev, I.B.; Suponitsky, K.Y.; Godovikov, I.A.; Bregadze, V.I. Synthesis of 10-methylsulfide and 10-alkylmethylsulfonium *nido*-carborane derivatives: B-H···π Interactions between the B-H-B hydrogen atom and alkyne group in 10-RC≡CCH_2S(Me)-7,8-$C_2B_9H_{11}$. *Eur. J. Inorg. Chem.* **2017**, 4436–4443. [CrossRef]
34. Anufriev, S.A.; Sivaev, I.B.; Suponitsky, K.Y.; Bregadze, V.I. Practical synthesis of 9-methylthio-7,8-*nido*-carborane [9-MeS-7,8-$C_2B_9H_{11}$]$^-$. Some evidences of BH···X hydride-halogen bonds in 9- XCH_2(Me)S-7,8-$C_2B_9H_{11}$ (X = Cl, Br, I). *J. Organomet. Chem.* **2017**, *849-850*, 315–323. [CrossRef]
35. Suponitsky, K.Y.; Tafur, S.; Masunov, A.E. Applicability of hybrid density functional theory methods to calculation of molecular hyperpolarizability. *J. Chem. Phys.* **2008**, *129*, 044109. [CrossRef]
36. Suponitsky, K.Y.; Masunov, A.E.; Antipin, M.Y. Conformational dependence of the first molecular hyperpolarizability in the computational design of nonlinear optical materials for optical switching. *Mendeleev. Commun.* **2008**, *18*, 265–267. [CrossRef]
37. Bader, R.F.W. *Atoms in Molecules. A Quantum Theory*; Clarendon Press: Oxford, UK, 1990.
38. Keith, T.A. *AIMAll (Version 15.05.18)*; TK Gristmill Software: Overland Park, KS, USA, 2015.
39. Espinosa, E.; Molins, E.; Lecomte, C. Hydrogen bond strengths revealed by topological analyses of experimentally observed electron densities. *Chem. Phys. Lett.* **1998**, *285*, 170–173. [CrossRef]
40. Espinosa, E.; Alkorta, I.; Rozas, I.; Elguero, J.; Molins, E. About the evaluation of the local kinetic, potential and total energy densities in closed-shell interactions. *Chem. Phys. Lett.* **2001**, *336*, 457–461. [CrossRef]
41. Lyssenko, K.A. Analysis of supramolecular architectures: Beyond molecular packing diagrams. *Mendeleev. Commun.* **2012**, *22*, 1–7. [CrossRef]
42. Suponitsky, K.Y.; Lyssenko, K.A.; Ananyev, I.V.; Kozeev, A.M.; Sheremetev, A.B. Role of weak intermolecular interactions in the crystal structure of tetrakis-furazano[3,4-c:3′,4′-g:3″,4″-k:3‴,4‴-o][1,2,5,6,9,10,13,14]octaazacyclohexadecine and its solvates. *Cryst. Growth Des.* **2014**, *14*, 4439–4449. [CrossRef]
43. Dmitrienko, A.O.; Karnoukhova, V.A.; Potemkin, A.A.; Struchkova, M.I.; Kryazhevskikh, I.A.; Suponitsky, K.Y. The influence of halogen type on structural features of compounds containing α-halo-α,α-dinitroethyl moieties. *Chem. Heterocycl. Comp.* **2017**, *53*, 532–539. [CrossRef]